

Strictly correlated uniform electron droplets

E. Räsänen,^{1,*} M. Seidl,² and P. Gori-Giorgi³¹*Nanoscience Center, Department of Physics, University of Jyväskylä, FI-40014 Jyväskylä, Finland*²*Institute of Theoretical Physics, University of Regensburg, D-93040 Regensburg, Germany*³*Department of Theoretical Chemistry and Amsterdam Center for Multiscale Modeling, FEW, Vrije Universiteit, De Boelelaan 1083, NL-1081HV Amsterdam, The Netherlands*

(Received 31 January 2011; published 9 May 2011)

We study the energetic properties of finite but internally homogeneous D -dimensional electron droplets in the strict-correlation limit. The indirect Coulomb interaction is found to increase as a function of the electron number, approaching the tighter forms of the Lieb-Oxford bound recently proposed by Räsänen *et al.* [*Phys. Rev. Lett.* **102**, 206406 (2009)]. The bound is satisfied in three-, two-, and one-dimensional droplets, and in the latter case it is reached *exactly*—regardless of the type of interaction considered. Our results provide useful reference data for delocalized strongly correlated systems, and they can be used in the development and testing of exchange-correlation density functionals in the framework of density-functional theory.

DOI: [10.1103/PhysRevB.83.195111](https://doi.org/10.1103/PhysRevB.83.195111)

PACS number(s): 71.15.Mb, 73.21.La, 31.15.eg, 71.10.Ca

I. INTRODUCTION

Strongly correlated materials have attracted tremendous interest across different fields of physics.¹ Famous examples of strongly correlated systems are high-temperature superconductors, organic conductors, ultracold atoms, and semiconductor quantum dots. These systems provide a particular challenge to theorists—simply because their properties cannot be predicted from the behavior of individual particles.

A physically important quantity in a quantum system is the magnitude of the indirect particle-particle interaction. This corresponds to the energy difference between the expectation value of the quantum mechanical interaction operator and the classical interaction energy of charged particles [see Eq. (2) below]. Lieb² showed that this quantity has a rigorous lower bound for Coulomb-interacting three-dimensional (3D) systems. Later on, the bound was tightened^{3,4} and extended to two-dimensional⁵ (2D) systems. In density-functional theory (DFT), this bound has been extensively used for building and testing approximations for the exchange-correlation energy functional (see, e.g., Refs. 6–8 and references therein).

More recently, using physical rather than formal arguments, an even tighter bound for 3D and 2D systems has been proposed together with an extension to one-dimensional (1D) systems.⁹ The basic idea of Ref. 9 is that the tightest form of the lower bound on the indirect interaction in D dimensions should correspond to the amount of correlation in the infinite D -dimensional homogeneous electron gas (HEG) in the low-density limit.^{8,9} This physically appealing idea provides an improved bound for 3D systems, the introduction of a relatively tighter bound in 2D, and a proposal for the bound in 1D.

Odashima and Capelle¹⁰ have shown through extensive numerical studies that *finite* electronic systems are energetically far above the lower bound, even when considering the tighter form of Ref. 9. This has triggered our interest to construct a finite yet physically simple system that is as close as possible to the bound of Ref. 9, or, if possible, even below (which would imply violation of the proposed lower bound). To challenge the bound maximally for a given density, the strict-interaction limit of DFT provides a suitable methodology. The mathematical structure of this approach—

corresponding to a system with a given density and maximum spatial correlation between the electrons—has been uncovered in the past three years.^{11–13} Consequently, explicit solutions, at least for centrally symmetric densities, have started to become available.^{14,15}

In this paper we use the strong-interaction limit of DFT to investigate the Lieb-Oxford bound in 3D, 2D, and 1D. We take the simplest imaginable test system, i.e., a finite D -dimensional electron droplet of a *uniform* density (up to a certain radius above which the density is rigorously zero) and examine its properties as the number of particles changes. Our analytic and numerical results show no evidence of violation of the lower bounds proposed in Ref. 9, but in all dimensions the low-density result of the HEG is approached as a function of the electron number N . In 1D, our large- N limit *exactly* corresponds to the proposed lower bound—regardless of the type of electron-electron interaction examined (contact, soft Coulomb, and regularized). In 2D and 3D, on the other hand, the large- N result is $\sim 2\%$ off the bound, although this small difference is within the errors associated with our numerical procedure.

II. THEORY

A. Lower bound on the indirect interaction

We consider a system of interacting electrons described by the Hamiltonian

$$\hat{H} = \hat{T} + \hat{V}_{ee} + \hat{V}_{\text{ext}}, \quad (1)$$

where \hat{T} is the kinetic-energy operator, \hat{V}_{ee} is the electron-electron (e - e) interaction, and \hat{V}_{ext} accounts for an external local one-body potential. We can define the *indirect* (quantum mechanical) part of the e - e interaction as

$$\tilde{W}[\Psi] \equiv \langle \Psi | \hat{V}_{ee} | \Psi \rangle - U[n_{\Psi}], \quad (2)$$

where

$$U[n] = \frac{1}{2} \int d\mathbf{r}' \int d\mathbf{r} n(\mathbf{r})n(\mathbf{r}')V_{ee}(|\mathbf{r} - \mathbf{r}'|) \quad (3)$$

is the classical (Hartree) interaction calculated from the (charge) density $n(\mathbf{r})$. In Eq. (2), $\Psi = \Psi(\mathbf{r}_1\sigma_1, \dots, \mathbf{r}_N\sigma_N)$ is

an arbitrary N -electron wave function (where σ_i denote spin variables) and $n_\Psi(\mathbf{r})$ is the density associated with it. The indirect e - e interaction has an important lower bound which can be expressed as

$$\tilde{W}[\Psi] \geq -C_D \int d^D r n_\Psi^{1/D+1}(\mathbf{r}), \quad (4)$$

where $D = 3, 2, 1$ is the dimension. In 3D, the bound originally found by Lieb² is best known as the Lieb-Oxford (LO) bound,³ having a prefactor $C_3^{\text{LO}} = 1.68$. The bound has been tightened by physical yet nonrigorous arguments to $C_3 = 1.44$.⁹ In 2D the existence of the bound was proven by Lieb, Solovej, and Yngvason⁵ (LSY) with $C_2^{\text{LSY}} = 192\sqrt{2\pi} \approx 481.28$. In Ref. 9, a tighter bound of $C_2 = 1.96$ was proposed.

The bound in Eq. (4) was originally constructed for Coulomb-interacting systems, where $\hat{V}_{ee} = \sum_{i < j} |\mathbf{r}_i - \mathbf{r}_j|^{-1}$. In 1D, however, this type of interaction is ill defined due to the divergence at $|x_i - x_j| = 0$. In Ref. 9 it was shown that a 1D bound can be constructed by applying a contact interaction or a soft-Coulomb interaction. In Sec. III C, the 1D case is studied in detail considering three types of the e - e interaction.

The bound of Eq. (4) can be equivalently expressed as^{6,8,10,16}

$$\lambda_D[\Psi] \equiv \frac{\tilde{W}[\Psi]}{E_x^{\text{LDA}}[n_\Psi]} \leq \frac{C_D}{A_D} \equiv \bar{\lambda}_D. \quad (5)$$

where

$$E_x^{\text{LDA}}[n] = -A_D \int d^D r n^{1/D+1}(\mathbf{r}) \quad (6)$$

is the local density approximation (LDA) for the electronic exchange energy, corresponding to the exact exchange energy for the HEG. Here the prefactors are given by $A_3 = 3^{4/3}\pi^{-1/3}/4$ and $A_2 = 2^{5/2}\pi^{-1/2}/3$ (for the 1D case see Sec. III C). In the right-hand side of Eq. (5), the values obtained for $\bar{\lambda}_D$ in 3D, 2D, and 1D are

$$\bar{\lambda}_3 = 1.96, \quad \bar{\lambda}_2 = 1.84, \quad \bar{\lambda}_1 = 2. \quad (7)$$

They have been proposed as the *tightest* bounds with the prefactors C_D given above—hence the bar symbol to differentiate from the functional $\lambda_D[\Psi]$. The upper bounds $\bar{\lambda}_D$ correspond to the low-density limit of the D -dimensional HEG. The physical argumentation⁹ behind the HEG result was motivated by the finding of Lieb and Oxford, who showed that there is a function $\tilde{\lambda}_3(N)$ which provides an upper bound for all systems with a particle number equal to N .^{3,17} The function $\tilde{\lambda}_3(N)$ is monotonic, with $\tilde{\lambda}_3(N+1) \geq \tilde{\lambda}_3(N)$, so that the most general bound of Eq. (5) is obtained by considering $N \rightarrow \infty$.

In this paper we focus on the question how the LO bound can be *challenged*. In other words, how must the wave function Ψ in Eq. (5) be chosen such that $\lambda_D[\Psi]$ becomes as large as possible? For any class of wave functions with a given fixed density $n(\mathbf{r})$,¹⁸ the answer to this question is

$$\max_{\Psi \rightarrow n} \lambda_D[\Psi] \equiv \Lambda_D[n] \equiv \frac{W_\infty[n]}{E_x^{\text{LDA}}[n]}, \quad (8)$$

where

$$W_\infty[n] \equiv \min_{\Psi \rightarrow n} \tilde{W}[\Psi] = \min_{\Psi \rightarrow n} \langle \Psi | \hat{V}_{ee} | \Psi \rangle - U[n] \quad (9)$$

is the indirect Coulomb energy in the strong-interaction limit of DFT, which can be now calculated (at least for centrally symmetric densities) with the theory of strictly correlated electrons.¹¹ This quantity was also considered in the original proof of the bound.^{2,3,6,8} In the following section we briefly review how the functional $W_\infty[n]$ of Eq. (9) can be constructed for a given density $n(\mathbf{r})$.

B. Strong-interaction limit

We may define $\Psi^\alpha[n]$ as the wave function that minimizes $\langle \Psi^\alpha | \hat{T} + \alpha \hat{V}_{ee} | \Psi^\alpha \rangle$ —corresponding to a system where the interaction is scaled—with the constraint of reproducing the given density $n(\mathbf{r})$. The scaled indirect Coulomb interaction $W_\alpha[n] = \langle \Psi^\alpha[n] | \hat{V}_{ee} | \Psi^\alpha[n] \rangle - U[n] \equiv \langle V_{ee}^\alpha \rangle - U[n]$ satisfies a set of useful exact relations within DFT.¹⁹

Here we consider the strong-interaction limit $\alpha \rightarrow \infty$, where it is sufficient to minimize the interaction term alone, since $\langle \alpha \hat{V}_{ee} \rangle$ grows faster than $\langle \hat{T} \rangle \propto \alpha^{1/2}$.^{12,20} As anticipated in Eq. (9), we thus compute explicitly, for a given density $n(\mathbf{r})$, the functional

$$\langle \hat{V}_{ee}^\infty \rangle \equiv \min_{\Psi \rightarrow n} \langle \Psi | \hat{V}_{ee} | \Psi \rangle. \quad (10)$$

In the strong-interaction limit of DFT the electrons minimize their interaction energy while reproducing the given *smooth* density $n(\mathbf{r})$. This $\alpha \rightarrow \infty$ limit is thus different from the more commonly considered Wigner crystal,²¹ as here the one-electron density is fixed *a priori* (and can be very different from the one of a Wigner-like structure, e.g., it can be the density of a weakly correlated system like a neutral atom¹¹). As discussed in detail in Refs. 11, 12, and 14, in the $\alpha \rightarrow \infty$ limit the relative positions of the electrons become strictly correlated: The position $\mathbf{r}_1 = \mathbf{r}$ of the first electron determines the positions \mathbf{r}_i of all the other electrons via $N-1$ *co-motion functions* $\mathbf{f}_i(\mathbf{r})$, $\mathbf{r}_i = \mathbf{f}_i(\mathbf{r})$. Thus, the probability of finding the first electron in the volume element $d\mathbf{r}$ around the position \mathbf{r} is the same as finding the i th electron in the volume element $d\mathbf{f}_i(\mathbf{r})$ around $\mathbf{f}_i(\mathbf{r})$, so that the co-motion functions are linked to the density through the differential equation $n(\mathbf{r})d\mathbf{r} = n[\mathbf{f}_i(\mathbf{r})]d\mathbf{f}_i(\mathbf{r})$, which has to be solved with the boundary condition that the corresponding expectation value of the interaction operator,¹¹

$$\langle \hat{V}_{ee}^\infty \rangle = W_\infty[n] + U[n] = \sum_{i=1}^{N-1} \sum_{j=i+1}^N \int d\mathbf{r} \frac{n(\mathbf{r})/N}{|\mathbf{f}_i(\mathbf{r}) - \mathbf{f}_j(\mathbf{r})|}, \quad (11)$$

is minimum.

Following Refs. 11 and 14, we consider here a spherical (circular) density in 3D and 2D, for which the $\mathbf{f}_i(\mathbf{r})$ can be constructed as follows. Given the expected number of electrons between 0 and r ,

$$N_e(r) = \int_0^r dr' S(r') n(r'), \quad (12)$$

where $S(r) = 4\pi r^2$ and $2\pi r$ in 3D and 2D, respectively, the general solution for the radial co-motion functions in a centrally symmetric N -electron system can be written as¹¹

$$f_{2k}(r) = \begin{cases} N_e^{-1}[2k - N_e(r)], & r \leq a_{2k}, \\ N_e^{-1}[N_e(r) - 2k], & r > a_{2k}, \end{cases} \quad (13)$$

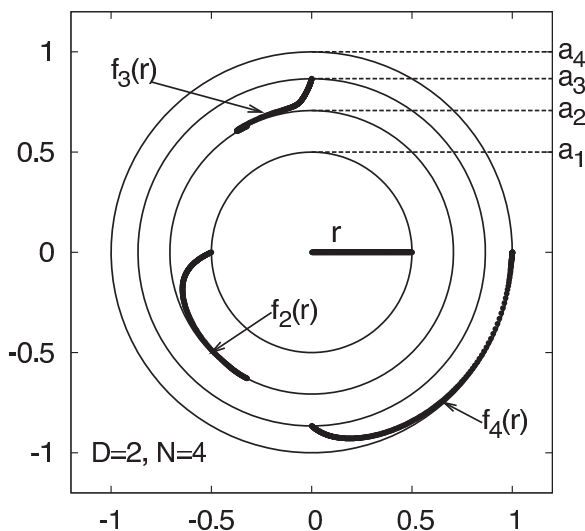


FIG. 1. Example of a section of the vectorial co-motion functions $\mathbf{f}_i(r)$ for a uniform droplet in two dimensions with $N = 4$ electrons. As the position of the first electron changes on the x axis from $x = 0$ to $x = a_1 = N_e^{-1}(1)$, the position of the second electron changes along the boldface curve from $r = a_2 = N_e^{-1}(2)$ to $r = a_1$, the position of the third electron from $r = a_2$ to $r = a_3 = N_e^{-1}(3)$, and the one of the fourth electron from $r = a_4 = N_e^{-1}(4)$ to $r = a_3$.

$$f_{2k+1}(r) = \begin{cases} N_e^{-1}[N_e(r) + 2k], & r \leq a_{N-2k}, \\ N_e^{-1}[2N - N_e(r) - 2k], & r > a_{N-2k}, \end{cases} \quad (14)$$

where $a_i = N_e^{-1}(i)$ and the integer k runs for odd N from 1 to $(N - 1)/2$, and for even N from 1 to $(N - 2)/2$. For even N , we need an additional function

$$f_N(r) = N_e^{-1}[N - N_e(r)]. \quad (15)$$

Equations (13)–(15) determine the distances $f_i(r)$ from the center of the remaining $N - 1$ electrons when, say, electron 1 is at a distance r from the center. The relative angles between the electrons, leading to the vectorial co-motion functions $\mathbf{f}_i(r)$, are determined by numerical minimization of Eq. (11) for each r . An example of such calculation for a 2D electron droplet of a uniform density with $N = 4$ electrons (see Sec. III B for more details) is shown in Fig. 1: As the position of the first electron changes on the x axis from $x = 0$ to $x = a_1 = N_e^{-1}(1)$, the position of the second electron changes along the boldface curve from $r = a_2$ to $r = a_1$, the one of the third electron from $r = a_2$ to $r = a_3$, and the one of the fourth electron from $r = a_4$ to $r = a_3$. The co-motion functions satisfy group properties such that the resulting e - e repulsion energy is invariant under exchange of two or more electrons, ensuring the indistinguishability of particles.^{11,14}

III. UNIFORM ELECTRON DROPLETS

A. Three dimensions

We consider a homogeneous N -electron droplet with a constant density n and a radius R . The density can then be expressed simply as

$$n(r) = \begin{cases} \frac{3N}{4\pi R^3}, & r \leq R, \\ 0, & r > R. \end{cases} \quad (16)$$

In a physical sense, this density and the corresponding wave function must be considered as limit cases (see the end of this section). The expected number of electrons between 0 and r is

$$N_e(r) = N \left(\frac{r}{R} \right)^3 \theta(R - r) + N\theta(r - R), \quad (17)$$

where θ is the Heaviside step function. The Hartree energy becomes

$$U[n] = \frac{1}{2} \int d\mathbf{r}' \int d\mathbf{r} \frac{n(\mathbf{r})n(\mathbf{r}')}{|\mathbf{r} - \mathbf{r}'|} = \frac{3N^2}{5R}, \quad (18)$$

and the LDA exchange energy [Eq. (6)] is

$$E_x^{\text{LDA}} = -\frac{3^{5/3}N^{4/3}}{28^{3/3}\pi^{2/3}R}. \quad (19)$$

For $N = 2$, we can readily test the accuracy of the LDA with respect to the exact exchange energy, $E_x^{\text{exact}}(N = 2) = -U(N = 2)/2$. We find $E_x^{\text{LDA}}/E_x^{\text{exact}} \approx 0.9621$. This ratio is expected to approach unity as $N \rightarrow \infty$.

The co-motion functions [Eqs. (13)–(15)] become

$$f_{2k}(r) = \left| \frac{2k}{N}R^3 - r^3 \right|^{1/3}, \quad (20)$$

$$f_{2k+1}(r) = \begin{cases} \left(\frac{2k}{N}R^3 + r^3 \right)^{1/3}, & r \leq R(1 - 2k/N)^{1/3}, \\ \left[\left(2 - \frac{2k}{N} \right) R^3 - r^3 \right]^{1/3}, & r > R(1 - 2k/N)^{1/3}, \end{cases} \quad (21)$$

and for even N we have to add the last function $f_N(r) = |R^3 - r^3|^{1/3}$. These co-motion functions keep the electrons in different spherical shells (each one containing, in the quantum mechanical problem, on average one electron—see the example of Fig. 1), while keeping the first derivative of the external potential continuous.¹¹ The expectation value of the e - e interaction in the strong-interaction limit can now be calculated from

$$\begin{aligned} \langle \hat{V}_{ee}^\infty(R) \rangle &= 4\pi \int_0^{a_1} dr r^2 n(r) V_{ee}[r, f_2(r), \dots, f_N(r), \Omega(r); R] \\ &= \frac{3N}{R^3} \int_0^{RN^{-1/3}} dr r^2 V_{ee}[r, f_2(r), \dots, f_N(r), \Omega(r); R], \end{aligned}$$

where we have used the fact that integrating between 0 and R is equivalent¹¹ to integrating N times between 0 and a_1 , where $a_1 = N_e^{-1}(1) = RN^{-1/3}$. The function $\Omega(r)$ denotes all the relative angles between the electrons as a function of r and is calculated numerically.¹¹ Changing variables $x = r/R$ leads to

$$\langle \hat{V}_{ee}^\infty(R) \rangle = 3N \int_0^{N^{-1/3}} dx x^2 V_{ee}[x, f_2(x), \dots, f_N(x), \Omega(x); R]. \quad (22)$$

Upon coordinate scaling it is easy to see that

$$\begin{aligned} &V_{ee}[x, f_2(x), \dots, f_N(x), \Omega(x); R] \\ &= \frac{1}{R} V_{ee}[x, f_2(x), \dots, f_N(x), \Omega(x); R = 1]. \end{aligned} \quad (23)$$

TABLE I. Calculated values for Λ_3 and Λ_2 as a function of the number of electrons N in uniform strictly correlated electron droplets in 3D and 2D, respectively.

N	Λ_3	Λ_2
1	1.310	1.414
2	1.498	1.556
3	1.550	1.607
4	1.603	1.644
5	1.627	1.666
6	1.657	1.679
7	1.672	1.692
10	1.708	1.719
14	1.733	1.736
20	1.761	1.743
30	1.784	1.758

Finally, we can write Eq. (8) as a function of N ,

$$\Lambda_3(N) = \frac{\langle \hat{V}_{ee}^\infty(R=1) \rangle - 3N^2/5}{-3^{5/3}\pi^{-2/3}(N/4)^{4/3}}, \quad (24)$$

where, as said, $\langle \hat{V}_{ee}(R=1) \rangle$ is calculated numerically. Special cases are $N=1$ and $N=2$, yielding analytic expressions. For a single electron $\langle \hat{V}_{ee} \rangle$ is trivially zero and we find $\Lambda_3(N=1) = 4(2\pi/3)^{2/3}/5 \approx 1.310$. For $N=2$ we get $\langle \hat{V}_{ee}(R=1) \rangle = 3(8 - 2^{1/3}\Gamma(1/6)\Gamma(4/3)/\sqrt{\pi})/20$, leading to $\Lambda_3(N=2) \approx 1.498$. Both values are lower than those given for $\tilde{\lambda}_3(N=1)$ and $\tilde{\lambda}_3(N=2)$ in Ref. 17.

Our numerical results for larger N are summarized in Table I. The results are also plotted (as circles) in Fig. 2. The curve intersecting the tabulated values has been obtained by

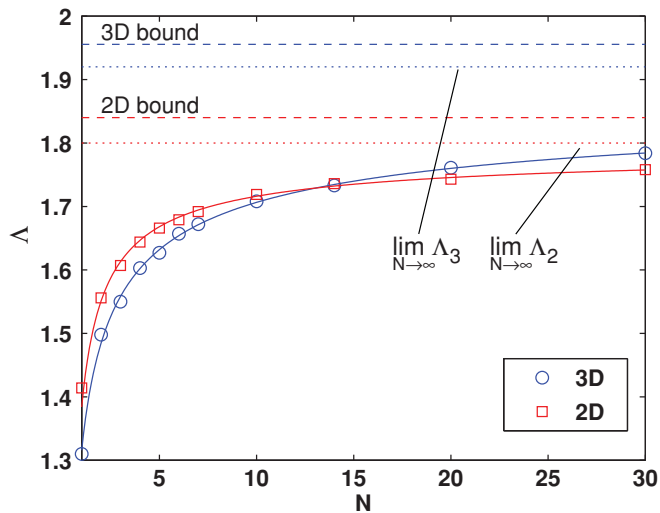


FIG. 2. (Color online) Values obtained for Λ_3 (circles) and Λ_2 (squares) as a function of the electron number N . The dotted lines show the estimated limit values for uniform electron droplets when N goes to infinity. The dashed lines show the bounds $\tilde{\lambda}_3$ and $\tilde{\lambda}_2$ for 3D and 2D systems, respectively, corresponding to the low-density limit of the homogeneous electron gas (Ref. 9).

numerical fitting of $\langle \hat{V}_{ee}^\infty(R=1) \rangle$ using a liquid-drop model expansion, which leads for $\Lambda_3(N)$ to the formula

$$\Lambda_3^{\text{fit}}(N) = -\frac{4}{3} \left(\frac{2\pi}{3} \right)^{2/3} (a_1 + a_2 N^{-1/3} + a_3 N^{-2/3}), \quad (25)$$

where $a_1 = -0.879717$, $a_2 = 0.153634$, and $a_3 = 0.123195$. When N goes to infinity, the fit yields a value $\Lambda_3(N \rightarrow \infty) \approx 1.92$ plotted as a dotted line in Fig. 2. This value is lower than the bound proposed in Ref. 9 for 3D systems corresponding to $\tilde{\lambda}_3 = 1.9555$ (dashed line). However, the difference is rather small ($\sim 2\%$) and it is actually within the error associated to the fitting procedure. Our values for $\Lambda_3(N)$ as well as our fitting curve are always below the model for $\tilde{\lambda}_3(N)$ proposed by Odashima *et al.*¹⁷

It should be noted that, per se, the density given in Eq. (16) corresponds to a nondifferentiable wave function due to the sharp edge at $r=R$. Therefore, it is important to examine whether the results above are valid when considering the density as a limit case of a physical density. A simple choice would be a density profile of the form of a Fermi function, i.e.,

$$\tilde{n}(r) = \frac{\text{const}}{e^{\alpha(r-R)} + 1}, \quad (26)$$

where the numerator is the normalization constant and the value for α determines the sharpness of the edge. The limit $\alpha \rightarrow \infty$ corresponds to the density of the form of Eq. (16). Figure 3 shows the values obtained numerically for Λ_3 with $N=1$ (bottom) and $N=2$ (up) as a function of α . From the figure it is clear that the (analytic) values corresponding to the original (sharp) density are approached as $\alpha \rightarrow \infty$; this is particularly convincing with $N=1$, where we can numerically

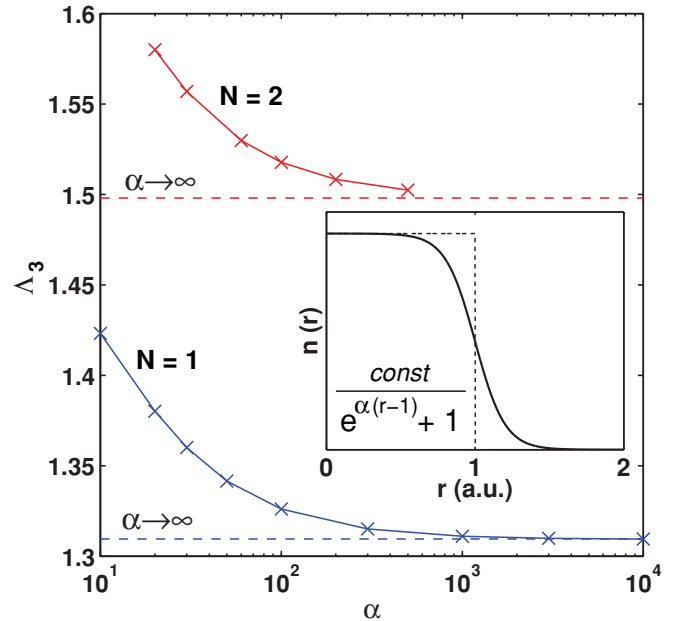


FIG. 3. (Color online) Values obtained for Λ_3 with $N=1$ (bottom) and $N=2$ (up) when a soft tail of the density (solid line in the inset) is applied. In the limit of a sharp edge (dashed line in the inset), corresponding to $\alpha \rightarrow \infty$, the results for the proposed homogeneous density droplet in Eq. (16) are reproduced (dashed lines).

study very large values for α (even several orders of magnitude larger than those shown in the figure). Thus, applying densities of the form of Eq. (16) can be seen as a limiting case for a quantum system.

B. Two dimensions

In 2D a homogeneous N -electron droplet with a radius R is defined by the density

$$n(r) = \begin{cases} \frac{N}{\pi R^2}, & r \leq R, \\ 0, & r > R, \end{cases} \quad (27)$$

and the expected number of electrons between 0 and r is

$$N_e(r) = N \left(\frac{r}{R}\right)^2 \theta(R-r) + N\theta(r-R). \quad (28)$$

The Hartree energy is more tricky to calculate than in 3D, since using Eq. (18) directly leads to an elliptic integral. However, we can use the fact that for a 2D disk with a radius r and a constant density n , the Hartree potential *at the rim* of the disk is $V_H = 4n r$ (Ref. 22). The Hartree energy is now equal to the work required to charge the disk from the center ($r = 0$) to the rim ($r = R$),

$$U[n] = \frac{N}{\pi R^2} 2\pi \int_0^R dr r V_H(r) = \frac{8N^2}{3\pi R}. \quad (29)$$

The LDA exchange energy is

$$E_x^{\text{LDA}} = -\frac{2^{5/2} N^{3/2}}{3\pi R}. \quad (30)$$

Again, for the special case of $N = 2$ we can compare E_x^{LDA} with the exact exchange energy, $E_x^{\text{exact}} = -U/2$. We find $E_x^{\text{LDA}}/E_x^{\text{exact}} = 1$, i.e., the LDA exchange energy is, by coincidence, exact for $N = 2$.

In 2D the co-motion functions have the same form as in 3D [Eqs. (20) and (21)] apart from the change in exponents as $3 \rightarrow 2$ and $1/3 \rightarrow 1/2$. The expectation value of the e - e interaction operator in the strong-interaction limit becomes

$$\langle \hat{V}_{ee}^\infty(R) \rangle = 2N \int_0^{N^{-1/2}} dx x V_{ee}[x, f_2(x), \dots, f_N(x), \Omega(x); R], \quad (31)$$

and after scaling of the distances we find

$$\Lambda_2(N) = \frac{\langle \hat{V}_{ee}^\infty(R=1) \rangle - 8N^2/(3\pi)}{-2^{5/2} N^{3/2}/(3\pi)}. \quad (32)$$

For $N = 1$ we get now simply $\Lambda_2(N = 1) = \sqrt{2}$, and the two-electron case yields $\Lambda_2(N = 2) = 2 - 3\pi\{8 + \sqrt{2}[\ln 2 + \ln(2 - \sqrt{2}) - 3\ln(2 + \sqrt{2})]\} \approx 1.556$. Results for larger N are given in Table I and Fig. 2. Interestingly, the 2D values are higher than the 3D ones at small N , but at $N \sim 15$ they go below the 3D curve. Again, we use a liquid-drop-model expansion to fit our data, leading to

$$\Lambda_2^{\text{fit}}(N) = -\frac{3\pi}{4\sqrt{2}}(b_1 + b_2 N^{-1/2} + b_3 N^{-1}), \quad (33)$$

with $b_1 = -1.0814$, $b_2 = 0.121609$, and $b_3 = 0.129014$. The large- N limit yields $\Lambda_2(N \rightarrow \infty) = 1.80$, which is, also in this case, $\sim 2\%$ lower than the 2D bound $\bar{\lambda}_2 = 1.84$ in Ref. 9.

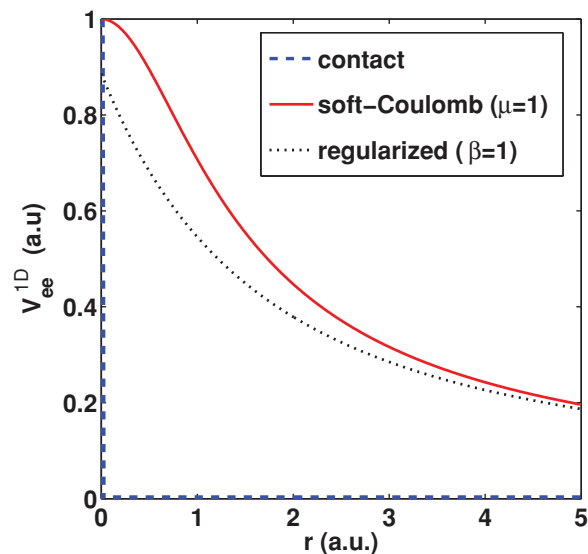


FIG. 4. (Color online) Different e - e interaction potentials considered for 1D systems.

C. One dimension

As mentioned in Sec. II A, the Coulomb interaction is ill defined in 1D. Various forms for physically reasonable 1D e - e interaction operators have been suggested, and below we focus on three of them: the contact, soft-Coulomb, and regularized interaction. The shapes of the interaction potentials are visualized in Fig. 4.

Regardless of the type of e - e interaction, the 1D homogeneous electron droplet has a density

$$n(x) = \begin{cases} \frac{N}{2R}, & |x| \leq R, \\ 0, & |x| > R, \end{cases} \quad (34)$$

and the expected number of electrons between $-\infty$ and x (here corresponding to the cumulative distribution function) is

$$N_e(x) = \int_{-\infty}^x dx' n(x') = \begin{cases} 0, & x < -R, \\ \frac{N}{2R}x + \frac{N}{2}, & |x| \leq R, \\ N, & x > R, \end{cases} \quad (35)$$

The co-motion functions $f_i(x)$ can be found in a straightforward fashion. When the first electron ($i = 1$) is set at $-R$, the electron i is located at $a_{i-1} = 2(i-1)R/N - R$. This leads to

$$f_i(x) = \begin{cases} N_e^{-1}[N_e(x) + i - 1], & x \leq N_e^{-1}(N + 1 - i), \\ N_e^{-1}[N_e(x) - (N + 1 - i)], & x > N_e^{-1}(N + 1 - i), \end{cases} \quad (36)$$

and after substituting N_e^{-1} we get

$$f_i(x) = \begin{cases} x + 2\frac{R}{N}(i-1), & x \leq 2\frac{R}{N}(1-i) + R, \\ x + 2\frac{R}{N}(i-1) - 2R, & x > 2\frac{R}{N}(1-i) + R. \end{cases} \quad (37)$$

The expectation value of the e - e interaction in the strong-interaction limit can be written as

$$\begin{aligned} \langle \hat{V}_{ee}^\infty(R) \rangle &= \int_{-\infty}^{\infty} dx \frac{n(x)}{N} \sum_{i>j} V_{ee}(|f_i(x) - f_j(x)|) \\ &= \sum_{i>j} V_{ee} \left(\left| 2 \frac{R}{N} (i - j) \right| \right), \end{aligned} \quad (38)$$

where we have replaced the full integral by N integrals between $-R$ and $a_1 = -R + 2R/N$, so that the difference between two co-motion functions is always $f_i(x) - f_j(x) = 2(i - j)R/N$. Thus, we notice that the strong-interaction limit in 1D, in the case of a *uniform* density, corresponds to the Wigner-crystal solution due to the translational invariance. In 3D and 2D instead, the distances between $f_i(r)$ always depend on r .

Next, let us write the Hartree energy and the LDA exchange energy in a general form,

$$U[n] = \frac{N^2}{8R^2} \int_{-R}^R \int_{-R}^R dx dx' V_{ee}(|x - x'|), \quad (39)$$

$$E_x^{\text{LDA}} = \int_{-\infty}^{\infty} dx n(x) \epsilon_x(n), \quad (40)$$

where the exchange energy per electron in a 1D HEG is²¹

$$\epsilon_x(n) = -\frac{1}{2\pi} \int_0^{2k_F} dq \tilde{V}_{ee}(q) \left(1 - \frac{q}{2k_F} \right). \quad (41)$$

Here \tilde{V}_{ee} is the Fourier transform of the e - e interaction and $k_F = \pi n/2$ is the Fermi vector in 1D. In the following, we will use the above general expressions to compute Λ_1 in Eq. (8) as a function of N .

1. Contact interaction

The contact (or delta) interaction is defined as

$$V_{ee}(x) = \eta \delta(x) \quad (42)$$

(see the dashed line in Fig. 4) and its Fourier transform is simply $\tilde{V}_{ee}(q) = \eta$, where η is a dimensionless constant. The Hartree energy [Eq. (39)] becomes

$$U[n] = \frac{\eta N^2}{4R}, \quad (43)$$

and the LDA exchange energy [Eq. (40)] is

$$E_x^{\text{LDA}} = -\eta \frac{N^2}{8R}. \quad (44)$$

We see that, in this case, the calculation of the constrained minimization of Eq. (10) does not have a unique minimizing wave function. Indeed, with the contact interaction the minimum value $\langle \hat{V}_{ee}^\infty \rangle = 0$ can be produced with any wave function that prevents the electrons to be at the same position while yielding the assigned density. The strictly correlated wave function is just one of those. Thus, we trivially obtain $\Lambda_1 = 2$, which is *independent of N* , and coincides with the lower bound $\bar{\lambda}_1$ of Ref. 9.

2. Soft-Coulomb interaction

The soft-Coulomb interaction is defined as

$$V_{ee}(x) = \frac{1}{\sqrt{x^2 + \mu^2}}, \quad (45)$$

where μ is the softening (or cutoff) parameter. The potential is visualized as a solid line in Fig. 4. Its Fourier transform is $\tilde{V}_{ee}(q) = 2 K_0(\mu q)$, where K_0 is the modified Bessel function of the second kind.²³ This expression leads to the LDA exchange energy of the form

$$\begin{aligned} E_x^{\text{LDA}} &= -\frac{N^2}{4R} \int_0^1 dx 2(1-x) K_0 \left(\frac{\pi \mu N}{2R} x \right) \\ &= -\frac{N^2}{4R} \left[\ln \left(\frac{4R}{\pi \mu N} \right) + \frac{3}{2} - \gamma \right] + O \left(\frac{\pi \mu N}{2R} \right)^2, \end{aligned} \quad (46)$$

where $\gamma \approx 0.577$ is Euler's constant. The leading term at small $\pi \mu N/(2R)$ agrees with the result of Fogler.²⁴

The calculation of the Hartree energy leads to a tedious integral but finally yields an analytic expression,

$$\begin{aligned} U[n] &= \frac{N^2}{4R} \left\{ \mu/R - \sqrt{4 + (\mu/R)^2} - \ln(\mu/R) \right. \\ &\quad \left. + \frac{1}{2} \ln \left[\frac{(\sqrt{4 + (\mu/R)^2} + 2)^3}{\sqrt{4 + (\mu/R)^2} - 2} \right] \right\} \\ &= \frac{N^2}{4R} \left\{ 4 \ln(2) - 2 - 2 \ln \left(\frac{\mu}{R} \right) + \frac{\mu}{R} - \frac{1}{8} \left(\frac{\mu}{R} \right)^2 \right. \\ &\quad \left. + \frac{1}{256} \left(\frac{\mu}{R} \right)^4 - \frac{1}{3072} \left(\frac{\mu}{R} \right)^6 + O \left(\frac{\mu}{R} \right)^8 \right\}, \end{aligned} \quad (47)$$

where we also give the series expansion for small values of (μ/R) , which is the regime of our primary interest (see below). Finally, the strong-interaction limit for the e - e interaction in Eq. (38) leads to

$$\langle \hat{V}_{ee}^\infty(R) \rangle = \frac{N}{R} \sum_{i>j}^N \frac{1}{\sqrt{4(i-j)^2 + \left(\frac{\mu N}{R} \right)^2}}. \quad (48)$$

Similarly to the 3D and 2D case, we may set $R = 1$. Thus, values for Λ_1 essentially depend on N and μ , and in E_x^{LDA} and $\langle \hat{V}_{ee}^\infty(R) \rangle$ also through their product $N\mu$. Hence, in the following we fix $N\mu$ and examine numerically the behavior of Λ_1 as a function of N . As visualized in Fig. 5, we find that increasing values for $N\mu$ lead to a decrease in Λ_1 , whereas decreasing $N\mu$ leads to an asymptotic approach of Λ_1 toward two. This tendency is in agreement with the bound $\bar{\lambda}_1 = 2$ in Ref. 9, where it was assumed that the LO-like bound in a *soft-Coulombic* 1D system has the same general form as Eq. (4) upon the multiplication of the logarithmic factor in Eq. (46).

3. Regularized interaction

As the third alternative for the e - e interaction in 1D we consider the regularized form of the Coulomb interaction in

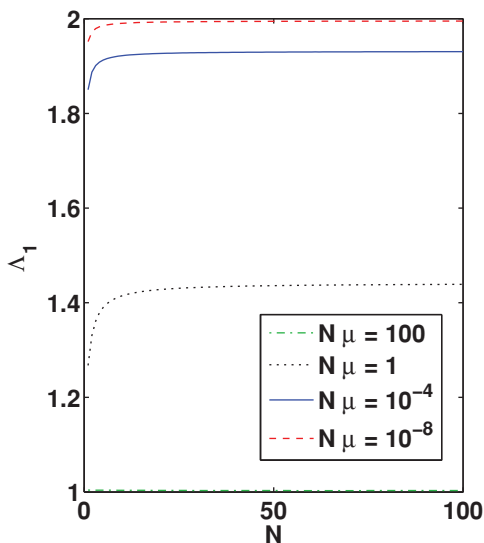


FIG. 5. (Color online) Values obtained for Λ_1 as a function of the electron number N with different values for $N\mu$, where μ is the softening parameter in the soft-Coulomb interaction.

1D. In particular, we take the representation of the Yukawa interaction in an infinite cylindrical wire of radius β .²¹ The system is then studied in the limit where the (finite) range of this interaction is larger than any other length scale except the length of the wire. The resulting interaction potential in the momentum space is²¹

$$\tilde{V}_{ee}(q) = e^{\beta^2 q^2} \text{Ei}(\beta^2 q^2), \quad (49)$$

where $\text{Ei}(z)$ is the exponential-integral function.²³ In real space the interaction can be written as

$$V_{ee}(x) = \frac{\sqrt{\pi}}{2\beta} e^{x^2/(4\beta^2)} \text{erfc}\left(\frac{|x|}{2\beta}\right), \quad (50)$$

where $\text{erfc}(z) = 1 - \text{erf}(z)$ is the complementary error function. The potential is visualized as a dotted line in Fig. 4.

As can be expected, all terms required to calculate Λ_1 become now rather cumbersome. The LDA exchange energy is

$$E_x^{\text{LDA}} = -\frac{N^2}{4R} \int_0^1 dq e^{q^2 b^2} \text{Ei}(-q^2 b^2)(1-q), \quad (51)$$

where $b = \pi\beta N/(2R)$. The Hartree integral is more straightforward to calculate in Fourier space. This leads to

$$\begin{aligned} U[n] &= \frac{1}{2\pi} \int_0^\infty dq \tilde{n}^2(q) \tilde{V}_{ee}(q) \\ &= \frac{N}{2\pi} \int_0^\infty dq \frac{\sin^2(qR)}{(qR)^2} \tilde{V}_{ee}(q) \\ &= \frac{\pi^{3/2}}{2} \left[\frac{\beta}{R} - \frac{\beta}{R} e^{R^2/\beta^2} + \sqrt{\pi} \text{erfi}\left(\frac{R}{\beta}\right) \right] \\ &\quad - \frac{1}{3} \frac{R^2}{\beta^2} {}_pF_q\left(1, 1; 2, \frac{5}{2}; \frac{R^2}{\beta^2}\right), \end{aligned} \quad (52)$$

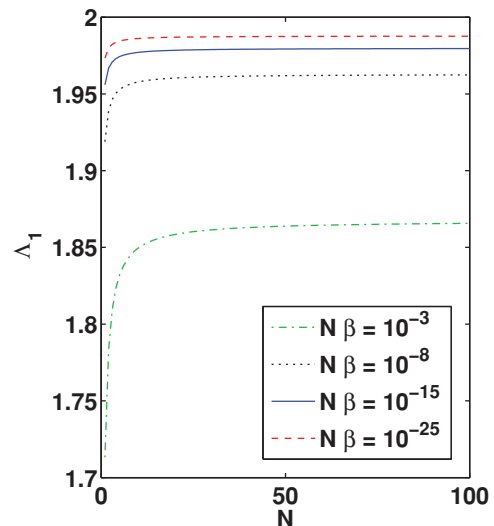


FIG. 6. (Color online) Values obtained for Λ_1 as a function of the electron number N with different values for $N\beta$, where β is the cutoff parameter in the regularized electron-electron interaction.

where erfi is the imaginary error function and ${}_pF_q$ is the generalized hypergeometric function.²³ The strong-interaction limit of the e - e interaction becomes

$$\langle \hat{V}_{ee}^\infty(R) \rangle = \frac{\sqrt{\pi}}{2\beta} \sum_{i>j}^N \exp\left[\frac{R(i-j)}{\beta N}\right]^2 \text{erfc}\left(\frac{R|i-j|}{\beta N}\right). \quad (53)$$

Now, to calculate Λ_1 for the regularized interaction using the quantities above, we have to restrict the parameter range. First, E_x^{LDA} in Eq. (51) is unstable for small b , and $U[n]$ in Eq. (52) is unstable for small β/R . Therefore, in both cases we numerically compute the series expansions up to the second order of these quantities. This corresponds to the physically justified small- β limit of the infinite cylinder. Second, $\langle \hat{V}_{ee}^\infty(R) \rangle$ is unstable for large $R|i-j|/(\beta N)$, so we again use the series expansion.

In Fig. 6 we show the behavior of Λ_1 as a function of N with different (small) values of $N\beta$. As in the soft-Coulombic case, decrease in the ‘‘cutoff’’ parameter in the e - e interaction leads to a tendency toward $\Lambda_1 = 2$, although in this case the approach is very slow as a function of $N\beta$. Nevertheless, the results are in line with other types of e - e interaction. It should be noted that for this regularized interaction a LO-like bound has *not* been constructed or even proposed before. Therefore, on the basis of our results above we may suggest $\bar{\lambda}_1 = 2$ for the bound, thus agreeing with 1D systems interacting through contact or soft-Coulomb interaction.

IV. CONCLUSIONS AND PERSPECTIVES

To summarize, we have examined the properties of strictly correlated electron droplets having a locally uniform density. In particular, we have used the theory of strictly correlated electrons to test the validity of the lower bounds proposed in Ref. 9 on the indirect electron-electron interaction in D -dimensional quantum systems. We have found that the bound is satisfied in all dimensions, although it is approached

as a function of the electron number. In 1D droplets the bound is reached asymptotically regardless of the type of electron-electron interaction considered in this work. In 2D and 3D, we obtain values being a few percent above the lower bounds.

Our results can be taken as useful reference data for future investigations of strongly correlated systems in general, as well as for the development and testing of exchange-correlation functionals in the framework of density functional theory. In

future work we plan to investigate different densities, trying to challenge the bound maximally, as well as trying to provide reference data to construct N -dependent bounds.¹⁷

ACKNOWLEDGMENTS

This work was supported by the Academy of Finland and by the Netherlands Organization for Scientific Research (NWO) through a Vidi grant.

*esa.rasanen@jyu.fi

¹J. Quintanilla and C. Hooley, *Phys. World* **22**, 32 (2009).

²E. H. Lieb, *Phys. Lett. A* **70**, 444 (1979).

³E. H. Lieb and S. Oxford, *Int. J. Quantum Chem.* **19**, 427 (1981).

⁴Garnet Kin-Lic Chan and N. C. Handy, *Phys. Rev. A* **59**, 3075 (1999).

⁵E. H. Lieb, J. P. Solovej, and J. Yngvason, *Phys. Rev. B* **51**, 10646 (1995).

⁶M. Levy and J. P. Perdew, *Phys. Rev. B* **48**, 11638 (1993).

⁷M. M. Odashima and K. Capelle, *Phys. Rev. A* **79**, 062515 (2009).

⁸J. P. Perdew, in *Electronic Structure of Solids '91*, edited by P. Ziesche and H. Eschrig (Akademie Verlag, Berlin, 1991).

⁹E. Räsänen, S. Pittalis, K. Capelle, and C. R. Proetto, *Phys. Rev. Lett.* **102**, 206406 (2009).

¹⁰M. M. Odashima and K. Capelle, *J. Chem. Phys.* **127**, 054106 (2007).

¹¹M. Seidl, P. Gori-Giorgi, and A. Savin, *Phys. Rev. A* **75**, 042511 (2007).

¹²P. Gori-Giorgi, G. Vignale, and M. Seidl, *J. Chem. Theory Comput.* **5**, 743 (2009).

¹³P. Gori-Giorgi, M. Seidl, and G. Vignale, *Phys. Rev. Lett.* **103**, 166402 (2009).

¹⁴P. Gori-Giorgi and M. Seidl, *Phys. Chem. Chem. Phys.* **12**, 14405 (2010).

¹⁵P. Gori-Giorgi, M. Seidl, and A. Savin, *Phys. Chem. Chem. Phys.* **10**, 3440 (2008).

¹⁶M. M. Odashima and K. Capelle, *Int. J. Quantum Chem.* **108**, 2428 (2008).

¹⁷M. M. Odashima, K. Capelle, and S. B. Trickey, *J. Chem. Theory Comput.* **5**, 798 (2009).

¹⁸M. Levy, *Proc. Natl. Acad. Sci. USA* **76**, 6062 (1979).

¹⁹M. Levy and J. P. Perdew, *Phys. Rev. A* **32**, 2010 (1985).

²⁰M. Seidl, *Phys. Rev. A* **60**, 4387 (1999).

²¹G. F. Giuliani and G. Vignale, *Quantum Theory of the Electron Liquid* (Cambridge University Press, New York, 2005).

²²See p. 67 in M. Seidl, Habilitation thesis, University of Regensburg; Eq. (2.26) in *Berkeley Physics Course* (McGraw-Hill, New York, 1965); p. 41 in Ref. 21; Eq. (13) in M. Seidl, J. P. Perdew, and M. Levy, *Phys. Rev. A* **59**, 51 (1999).

²³M. Abramowitz and I. Stegun, *Handbook of Mathematical Functions* (Dover, New York, 1965).

²⁴M. M. Fogler, *Phys. Rev. Lett.* **94**, 056405 (2005).